Design of an all-solid-state photonic crystal fiber operating at wavelength 1 550 nm

Song Zhaoyuan[1], Liu Xiaodong[2], Zhang Siyuan[1], Huang Jinhua[1], Zhang Leilei[1]

(1. College of Science, Liaoning Shihua University, Fushun 113001, China;
2. College of Science, Tianjin Polytechnic University, Tianjin 300387, China)

Abstract: Numerical simulations were performed on the photonic band gap (PBG) properties of the photonic crystal fibers (PCFs) possessing a clad with the cladding holes triangle-lattice distributed and a round fiber core using the full-vector plane-wave expansion method. Through the comparative analysis on the relationship of the PBG property and the structure parameters (cladding hole diameter d_{clh}, cladding hole pitch Λ and cladding hole filling ration f) between traditional (air-silica) and all-solid-state (nonair-silica) PCFs, a design of an all-solid-state PCF was given out which operates at the communication wavelength of 1 550 nm with the parameters d_{clh}=1.0 μm, Λ=2.0 μm and f=0.23 at the conditions of fiber core diameter d_{co}=5.3 μm and cladding hole material′s refractive index n_{clh}=1.65. Further numerical simulation shows that this resulting PCF has a gap width up to 43 nm.

Key words: photonic crystal fiber; photonic band gap; full-vector plane-wave expansion method; all-solid-state

CLC number: TN929.11 **Document code:** A **Article ID:** 1007-2276(2015)04-1354-05

工作在 1 550 nm 的全固态光子晶体光纤的设计

宋昭远[1],刘晓东[2],张思远[1],黄金华[1],张磊磊[1]

(1. 辽宁石油化工大学 理学院,辽宁 抚顺 113001; 2. 天津工业大学 理学院,天津 300387)

摘 要: 利用全矢量平面波展开法对三角形排布孔包层-圆纤芯结构的光子晶体光纤的光子带隙特性进行了数值模拟,对比研究了传统光子晶体光纤(空气-石英纤芯结构)和全固态光子晶体光纤(非空气-石英纤芯结构)的光子带隙(导模)与结构参数(包层孔直径 d_{clh}、包层孔间距 Λ 和包层孔填充比 f)的关系,设计出了一组合适的结构参数(纤芯直径 d_{co}=5.3 μm,包层孔材料的折射率 n_{clh}=1.65,d_{clh}=1.0 μm,Λ=2.0 μm,f=0.7),可以使相应的全固态光子晶体光纤工作在 1 550 nm 的现代光通信波长上,且光子带隙可以达 100 nm。

关键词: 光子晶体光纤; 光子带隙; 全矢量平面波展开法; 全固态

收稿日期:2014-08-07; **修订日期**:2014-09-11

基金项目:国家自然科学基金青年基金(21403101);辽宁省自然科学基金(2013020151);抚顺市科学技术发展资金计划(20141117)

作者简介:宋昭远(1967-),男,副教授,博士,主要从事特种光纤及稀土掺杂光电材料方面的研究。Email:zysong815@163.com

0 Introduction

Traditional photonic crystal fibers (PCFs) which are called holey fibers or microstructured fibers, reported first more than twenty years ago[1], and many developments have been achieved till now[2-8], because of the transmission loss, dispersion and nonlinear effects in traditional fibers. With the continuing improvement of the optical fiber drawing technology, the quality of PCFs is becoming more and more perfect although its transmission loss is still more than that of traditional fibers, and it is easy to achieve a loss of 2 dB/km operating at 1 620 nm[3].

At present, the main pattern of the PCFs is based on the air-silica (quartz) structure, but the so-called all-solid-state (i.e., nonair-silica structure) PCF possessing a clad with nonair cladding holes (CHs, are so called although they are filled with nonair semiconductor functional materials) and a silica fiber core may have more advantages as a semiconductor optoelectronic device such as an optical fiber sensor working at 1 550 nm and is studied rarely.

This paper will design an all-solid-state PCF operating at the communication wavelength 1 550 nm through the comparative analysis on the relationship of the PBG property and the structure parameters between the traditional (air-silica) and all-solid-state (nonair-silica) PCFs by using of the full-vector plane-wave expansion method[9-10].

1 Relationship of the PCBs and the structural parameters

The microstructure of the PCF possessing a clad with the CHs triangle-lattice distributed and an effective round fiber core (silica, its refractive index n_{co}=1.45 is the same as the background the CHs are embedded in) is schematically shown in Fig.1. In this figure the structural parameters the effective core diameter d_{co}, the CH diameter d_{clh}, the CH pitch Λ are defined schematically. For given parameters d_{clh} and Λ ($d_{clh} \leqslant \Lambda$), one can get a filling ratio:

$$f=\frac{\pi}{2\sqrt{3}}\cdot\left(\frac{d_{clh}}{\Lambda}\right)^2\approx 0.91\left(\frac{d_{clh}}{\Lambda}\right)^2 \quad (1)$$

Especially for the most closed packing situation $d_{clh}=\Lambda$, $f\approx 0.91$.

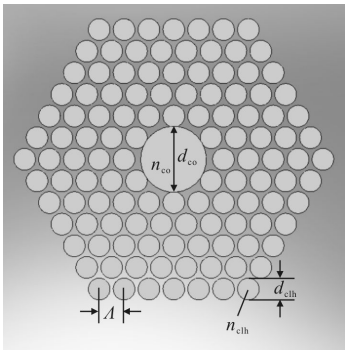

Fig.1 Cross section of the studied PCF with parameters defined in the figure

1.1 Effect of variable CH diameters on the PBGs

By using the full-vector plane-wave expansion method[9], the PBG properties as the function of the CH diameter d_{clh} ($1.0 \leqslant d_{cl} \leqslant 4.0$ μm) of the PCF with d_{co}=10.6 μm and Λ=4.0 μm are shown in Fig.2 (a) and (b) for n_{clh}=1 (the refractive index of the air) and n_{clh}=1.65 (the refractive index of some kind of solid state functional material), respectively.

From Fig.2 (a), it can be seen that when the air CH diameter d_{clh}=1.0−2.4 μm, the first PBG appears, but is narrow, which means the small air CHs are not prone to the formation of a PBG. When the air CH diameter d_{clh}=2.4−3.4 μm, up to 5 PBGs are formed and their center frequencies become higher. Nevertheless when d_{clh}>3.5 μm, the PBG number becomes fewer.

On the contrary, if the CHs are filled with a kind of nonair material whose refractive index n_{clh} > 1.45, the situation will be very different, as shown as Fig.2(b) for n_{clh}>1.65. From Fig.2(b), one can see that the first PBG begins to appear at only d_{clh}=0.5 μm and the PBG width is also large, while the number of PBGs is fewer and their center frequencies become lower.

From Fig.2, it is found that the central

wavelength of each PBG of both kinds of PCFs lies in the range of 2.0−2.2 μm.

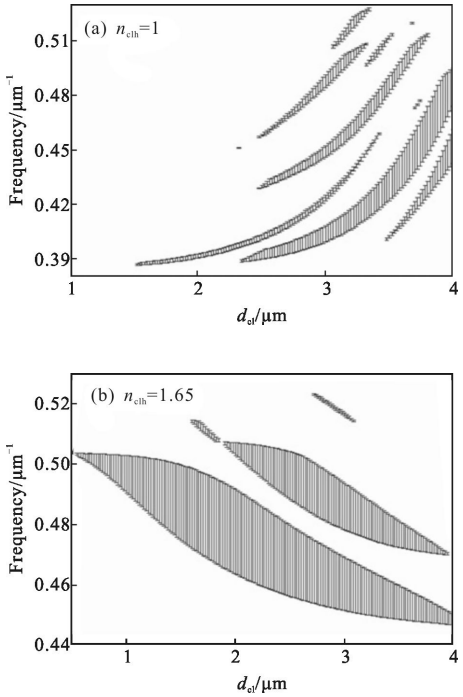

Fig.2 PBG property as the function of the CH diameter d_{cl}($1.0 \leqslant d_{cl} \leqslant 4.0$ μm) for the PCF with d_{co}=10.6 μm, Λ=4.0 μm and (a) n_{clh}=1, (b) n_{clh}=1.65

1.2 Effect of variable pitches on the PBGs

If given d_{co}=10.6 μm and d_{clh}=3.0 μm, the PBG property as the function of pitch Λ($3.0<\Lambda<10$ μm) for the PCF with n_{clh}=1 and n_{clh}=1.65 are shown in Fig.3(a) and (b), respectively.

From Fig.3, we can seen that for both kinds of PCFs, PBGs exist at small pitches, but they become narrower and their central wavelengths are all larger than about 1 600 nm with increasing the pitches. This can be demonstrated qualitatively by the fact that the difference between the silica core′s n_{co}=1.45 and the cladding′s effective refractive index approaches to zero for both kinds of PCF. Therefore it is concluded that the proper range of pitch Λ is less than two times of the CH diameter, although there are still three PBGs at Λ>7.0 μm because these PBGs are the in-plane type and therefore no guided mode occurs.

It is worthy noting that there are three PBGs with three respective constant cental frequencies for the second PCFs.

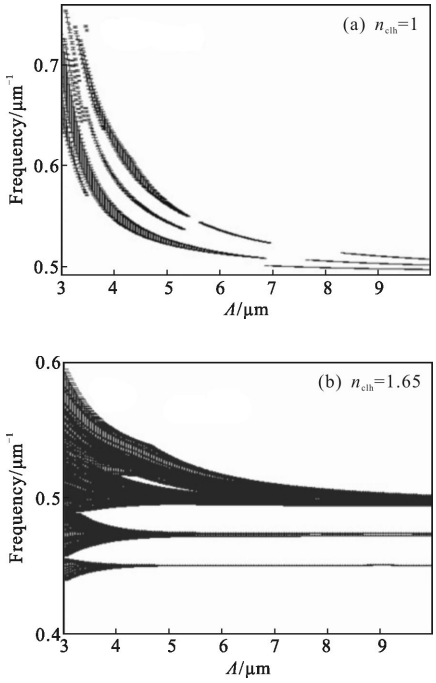

Fig.3 PBG property as the function of pitch Λ($3.0<\Lambda<10$ μm) for the PCF with d_{co}=10.6 μm, d_{clh}=3.0 μm and (a) n_{clh}=1, (b) n_{clh}=1.65

1.3 Effect of filling ratios on the PBGs

When discussing the effect of CH diameters d_{clh} on PBGs for a given pitch Λ, one can see that it is equivalent to analysis on the filling ration f − dependence of PBG property because of Eq. (1), whereas the latter is more intuitionistic. Fig.4 shows PBG property as the function of filling ratio f ($0.1<f<0.91$) for the PCF with d_{co}=10.6 μm, Λ=4.0 μm and n_{clh}=1.0 and n_{clh}=1.65, respectively.

From Fig.2 and 4, one can see that PBG properties exhibited in two sets of figures are really consistent with each other.

For the air-silica PCF, it is proper when the filling ratio f is larger than 0.3, while f>0.2 can already form two well-separated PBGs although their central wavelengths are still larger than 2.0 μm.

As to the nonair-silica PCF, it is not always better when the filling ratio is very large, because the central frequency becomes smaller and narrower when

f approaches to 0.91.

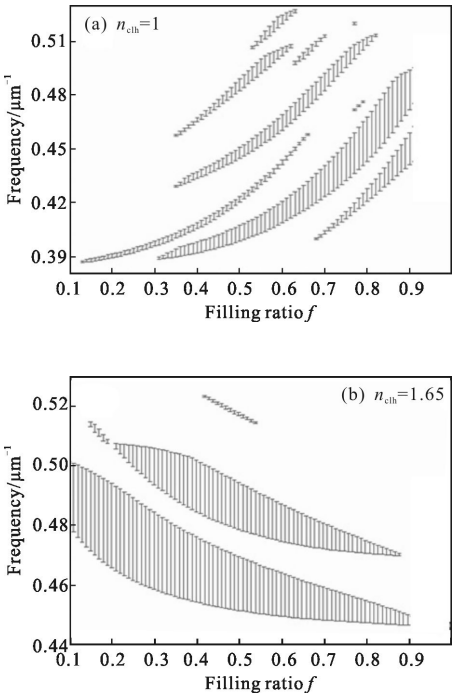

Fig.4 PBG property as the function of filling ratio f($0.1<f<0.91$) for the PCF with d_{co}=10.6 μm, Λ=4.0 μm and (a) n_{clh}=1, (b) n_{clh}=1.65

1.4 Comparative analysis on two kinds of PCFs

From the above-mentioned calculations and discussion, one can come to the following conclusion.

In a general air-silica PCF, the PBG width usually increases with enlarging the CH diameter d_{clh} and the entire PBG moves to the short-wave direction, while the PBG width usually decreases with expanding the CH pitch Λ and the entire PBG moves to the long-wave direction.

For an all-solid-state PCF, the results are completely opposite compared to the general air−silica one. The reason is just the symmetrically complement structures of the refractive index distributions for two kinds of PCFs, as shown as in Fig.5. Speaking theoretically, the PBG bound bends to the direction of the high−refractive index material for the former PCF, while to the reverse direction for the latter one, and therefore opposite effects appear for two kinds of PCFs although the cores are same in our PCFs.

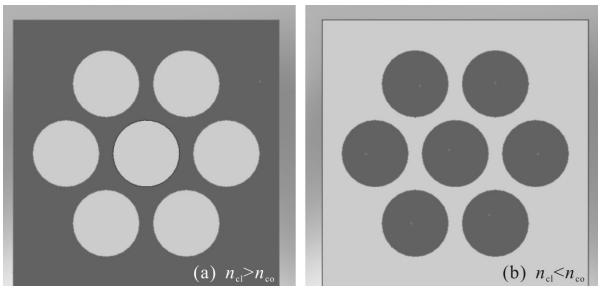

Fig.5 Complement structures of the refractive index distributions for two kinds of PCFs, where the deep green medium has a higher refractive index

2 Design of an all-solid-state PCF operating at wavelength 1550 nm

Based on the comparative analysis of the all-solid-state PCF with the air-silica PCF, we design an all-solid-state PCF that may have a conductive mode of 1 550 nm, whose parameters are n_{co}=1.45, d_{co}=5.3 μm, n_{clh}=1.65, d_{clh}=1.0 μm and Λ=2.0 μm. Figure 6 shows the relationship between normalized frequency ka (k is the free-space wave vector quantity $2\pi/\lambda$, $a=d_{co}/2=2.65$ μm is the effective core radius) and normalized propagation constant $\beta\Lambda$ (phase change in a length range of one pitch along the PCF).

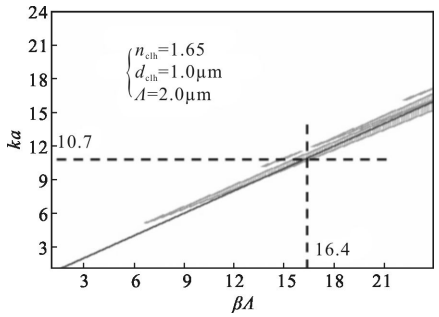

Fig.6 Relationship between normalized frequency ka and normalized propagation constant $\beta\Lambda$ along the PCF whose parameters are demonstrated in the text

From the relationship between k and wavelength λ, one can get:

$$ka=\frac{2\pi a}{\lambda}=\frac{2\pi d_{co}}{\lambda} \tag{2}$$

For λ_0=1 550 nm and d_{co}=5.3 μm, ka=10.7, there is really a conductive mode of 1 550 nm, as shown in Fig.6.

Furthermore, one can find out that the corresponding normalized propagation constant $\beta\Lambda$=16.4 from Fig.6, and therefore the propagation constant β=8.2 μm^{-1}. Figure 7 shows the relationship between the normalized frequency *ka* and the wave vector.

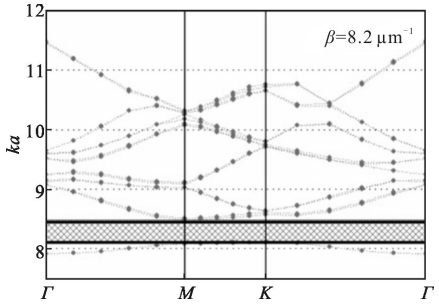

Fig.7 Relationship between the normalized frequency *ka* and the wave vector

From Fig.7, we obtain the PBG width $\Delta(ka)\approx 0.3$, and then the width of the 1 550 nm conductive mode will be

$$\Delta\lambda=\frac{\lambda^2\Delta(ka)}{2\pi a}\approx 0.043\ \mu\text{m} \tag{3}$$

It is worthy noting that this structure is very easy to be realized nowadays.

3 Conclusion

Through the comparative analysis on the relationship of the photonic band gap property and the structure parameters between the traditional (air-silica) and all-solid-state (nonair-silica) photonic crystal fibers by using of numerical simulations, we have designed an all-solid-state photonic crystal fiber operating at the communication wavelength 1 550 nm (width 43 nm) with the structural parameters d_{clh}=1.0 μm, Λ=2.0 μm and f=0.23 at the conditions of silica fiber core diameter d_{co}=5.3 μm and n_{clh}=1.65.

References:

[1] Ferrarini D, Vincetti L, Zoboli M, et al. Leakage properties of photonic crystal fibers [J]. ***Optics Express***, 2002, 10(23): 1314-1319.

[2] Knight J C, Birks T A, Russel J, et al. All-silica single-mode optical fiber with photonic crystal cladding [J]. ***Optics Letters***, 1996, 21(19): 1547-1549.

[3] Zhou Y Y, Zhou X J. New development and applications of photonic crystal fibers [J]. ***Optical Communication Technology***, 2007, 12 (5): 58-60.

[4] Florian J, Fabian S, Cesar J, et al. Avoided crossings in photonic crystal fibers [J]. ***Optics Express***, 2011, 19(14): 13578-13589.

[5] Song Zhaoyuan, Huang Jinhua, Zhang Leilei. Design of triple-cladding photonic crystal fiber with near-zero flattened dispersion [J]. ***Infrared and Laser Engineering***, 2014, 43(3): 823-827. (in Chinese)

[6] Li Shuguang, Zhu Xingping, Xue Jianrong. Supercontinuum generation in all-normal dispersion photonic crystal fiber[J]. ***Acta Physica Sinica***, 2013, 62 (20): 204206. (in Chinese)

[7] Cao Fengzhen, Zhang Peiqing, Dai Shixun, et al. Dispersion properties of chalcogenide glass photonic crystal fiber for mid-IR supercontinuum spectrum generation[J]. ***Infrared and Laser Engineering***, 2014, 43(4): 1150-1155. (in Chinese)

[8] Butler J J, Bowcock A S, Sueoka S R, et al. Optical properties of solid-core photonic crystal fibers filled with nonlinear absorbers[J]. ***Optics Express***, 2013, 21(18): 20707-20712.

[9] Liu Zhaolun, Wang Wei, Liu Xueqiang. Numerical simulation and experimental investigation of photonic bandgap photonic crystal fibers with interstitial holes [J]. ***Microwave and Optical Technology Letters***, 2012, 54 (1): 233-236.

[10] Chen Yue′e, Shao Qiufeng, Wang Jinsheng. Coherent beam combination of integrated photonic crystal fiber [J]. ***Infrared and Laser Engineering***, 2014, 43(5): 1454-1457. (in Chinese)